Available online at www.sciencedirect.com
ScienceDirect
Thin Solid Films 516 (2007) 454–459
www.elsevier.com/locate/tsf

Thickness-dependent microstructures and electrical properties of $CaCu_3Ti_4O_{12}$ films derived from sol–gel process

Li-Chun Chang [a,b], Dai-Ying Lee [c], Chia-Cheng Ho [c], Bi-Shiou Chiou [c,d,*]

[a] Department of Electronic Engineering, Huafan University, Taipei County, Taiwan
[b] Advanced Manufacturing Research Center, Huafan University, Taipei County, Taiwan
[c] Institute of Electronics, National Chiao-Tung University, Hsinchu, Taiwan
[d] Innovative Packaging Research Center, National Chiao-Tung University, Hsinchu, Taiwan

Available online 1 August 2007

Abstract

$CaCu_3Ti_4O_{12}$ (CCTO) thin films with various thicknesses were prepared by a sol–gel multiple coating processes on Pt/Ti/SiO_2/Si substrates. Microstructures and surface morphologies of CCTO thin films were analyzed by grazing incident X-ray diffractometer (GIXRD) and scanning electron microscope (SEM), respectively. The correlation between the thickness and electrical properties of CCTO films was investigated. The dielectric constants of CCTO films decreased with increasing film thickness (coating cycle). Both the dielectric constant of CCTO films and interlayer are calculated. Possible mechanisms are explored to explain the thickness dependence of the dielectric constant of CCTO films.
© 2007 Elsevier B.V. All rights reserved.

Keywords: Sol–gel; $CaCu_3Ti_4O_{12}$ (CCTO); Thickness-dependent properties; Dielectric

1. Introduction

Recently, the new pervoskite-type material $CaCu_3Ti_4O_{12}$ (CCTO) has attracted much attention because of its high dielectric constant over a broad temperature range. Each successive dynamic random access memories (DRAM) generation has to maintain the same storage charge, while the area of the capacitor has significantly decreased [1–6]. CCTO is a promising candidate for application of DRAM in very large scale integrated (VLSI) circuits due to its large dielectric constant. With the shrinking of device dimensions, high dielectric constant materials become more important and necessary to be used for capacitor in DRAM. Increasing the dielectric constant of the material or the area of a capacitor can achieve a large capacitance.

The high dielectric constant is attributed to the grain-boundary capacitance (internal barrier layer capacitance, IBLC) instead of an intrinsic property associated with the crystal structure [7]. In order to apply CCTO in microelectronic devices and give a more fundamental understanding of its physical property, some groups have grown CCTO films by pulsed-laser deposition (PLD) with different substrates [8,9]. In the work of Jiang et al., high quality epitaxial CCTO films were prepared on a (001)-oriented $LaAlO_3$ substrate and presented a high dielectric constant of 10^4 at 1 MHz at room temperature [8]. While in the studies of Fang and Shen, the CCTO thin film deposited on Pt/Ti/SiO_2/Si substrates showed a polycrystalline characteristic and achieved a dielectric constant of near 2000 at 10 kHz and room temperature [9,10]. The process window of the above methods of CCTO thin film is very narrow. In addition, the PLD method for CCTO is expensive. Sol–gel was chosen as the preparation technique in this study because it offers a homogeneous distribution of elements on a molecular level, ease of composition control, high purity, and the ability to coat large and complex area substrate. Both the dielectric constants of CCTO films and interlayer are calculated by Mixture Rule. A pore fraction of dielectric film is also estimated.

2. Experimental procedures

The CCTO thin films were prepared by a sol–gel technique. Four inch diameter p-type (100) Si wafers with nominal resistivity of 5 to 10 Ω cm were used as substrates. After standard RCA cleaning, a 200 nm SiO_2 film was grown on Si substrate, then 10 nm Ti and 100 nm Pt layers were deposited sequentially by dc

* Corresponding author. Institute of Electronics, National Chiao-Tung University, Hsinchu, Taiwan.
E-mail address: bschiou@mail.nctu.edu.tw (B.-S. Chiou).

0040-6090/$ - see front matter © 2007 Elsevier B.V. All rights reserved.
doi:10.1016/j.tsf.2007.07.009

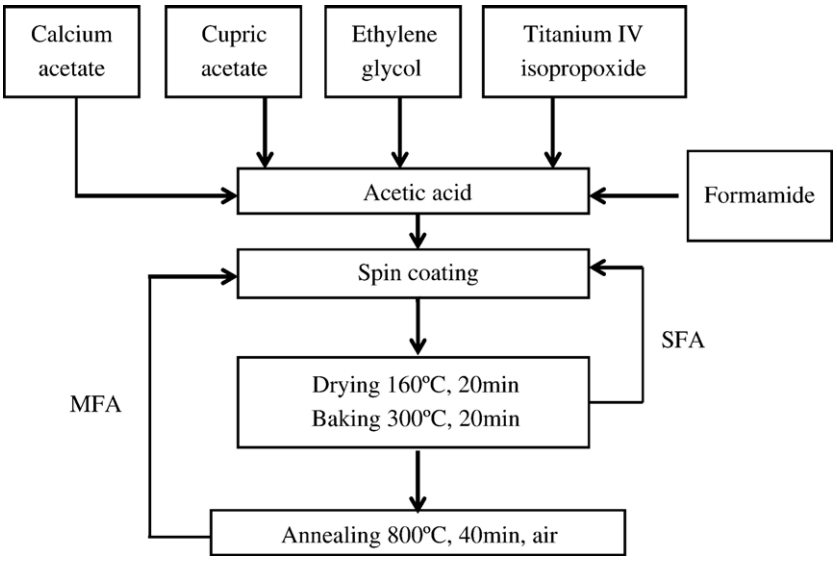

Fig. 1. Flow chart for the fabrication of CCTO films.

sputtering to obtain a Pt/Ti/SiO_2/Si substrate for the deposition of CCTO thin-film capacitors. Fig. 1 shows the flow chart of CCTO thin film fabrication. Precursor solution of CCTO with a 0.18 molar concentration was prepared by dissolving the appropriate amount of calcium and cupric acetates in acetate acid, and then it was added a stoichiometric amount of titanium IV isopropoxide. Following, ethylene glycol was added into the CCTO solution to increase solution stability. Formamide was selected as an additive to adjust the solution viscosity to prevent the cracking of CCTO thin films during baking. Then, the CCTO solution was heated at 165 °C for 80 min.

After the synthesis of CCTO solution is completed, the solution was spun-coated onto Pt/Ti/SiO_2/Si substrate at 7000 rpm for 30 sec. The CCTO thin films were baked at 160 °C for 20 min to dry the gel, and then heated in a furnace at 300 °C for 20 min to remove residual organic compounds. After the heating of the first CCTO film, a second CCTO film was spun, baked, and heated as described above. The process was repeated and CCTO thin films with different coating layers were obtained in order to avoid through pin-hole. Then, the CCTO films, denoted single-cycle furnace annealing (SFA) samples, were annealed at 800 °C in a furnace for 40 min with various thicknesses. Alternative preparation is the multi-cycle furnace annealing (MFA) specimens, each CCTO layer is spun, baked, heated, and annealed, and then the following deposition layer process is performed. Finally, the top electrodes of the Pt (100 nm) were deposited by DC sputtering system through a shadow mask.

A Setaram-Labsys thermogravimetric analyzer (TGA) and a Setaram-Labsys differential scanning calorimeter (DSC) were employed to measure the decomposition and crystallization temperatures of CCTO gel films. Both TGA and DSC experiments were carried out in a dry air atmosphere with a heating rate of 10 °C/min.

The phase of the films was characterized by a grazing incident X-ray diffractometer spectra collected by using CuK_α (λ=0.15406 nm) radiation with 40 kV and 150 mA in the 2θ range of 30 ° to 65 °(XRD, RU-H3R, Rigaku Co.). The cross sections of films were observed with a scanning electron microscope (SEM, Hitachi S4700). The capacitance was measured with a *C–V* analyzer (model 590, Keithley Instruments Inc.) in the applied voltage range of -5 ± 5 V and at the frequency of 100 kHz. An electron probe microanalyzer (FE-EPMA, JXA-8500F) was used to analyze the composition of the films.

3. Results and discussion

3.1. Microstructure

The TGA/DSC graphs of the CCTO films are shown in Fig. 2. The DSC curve exhibits two endothermic peaks and one exothermic peak. The first endothermic peak at 60 °C records the rapid volatilization of water in the gel. The presence of an exothermic peak at 250 °C is concerned with the decomposition of organic compound. In the meantime, a significant weight loss due to the evaporation of water and decomposition of organic compound is observed in the TGA curve for the temperature below 300 °C. The second endothermic peak at 765 °C in the DSC curve is related to the phase formation of perovskite CCTO,

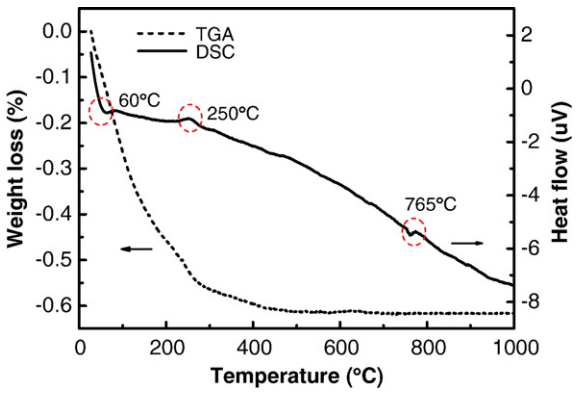

Fig. 2. TGA and DSC of the CCTO gel films heated in a dry air atmosphere at 10 °C/min.

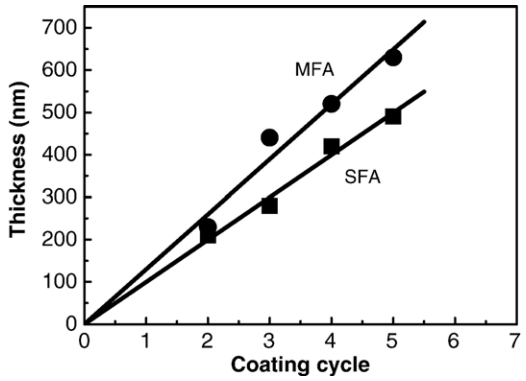

Fig. 3. Thickness of CCTO films vs. the coating cycle. ■: SFA, single-cycle furnace annealed at 800 °C, ●: MFA, multi-cycle furnace annealed at 800 °C.

while no weight change is detected in the TGA curve. Thus, 800 °C is set as the annealing temperature in this study.

The CCTO films prepared by SFA process with deposition layer numbers 2, 3, 4, and 5 possess 210, 280, 420, and 490 nm in thickness, respectively. While in the MFA process, the film thicknesses are 230, 440, 520, and 630 nm. Fig. 3 shows the relationship of film thickness and deposition layer number. The CCTO thickness versus the coating cycle shows linearity, and the slope is about 99.1 and 129.8 for SFA and MFA processes, respectively. Fig. 4 shows the SEM micrograph of the free surface of CCTO film annealed at 800 °C. The morphology presents the grains distribute in two categories, one size below 50 nm and another one above 300 nm, which implies the existence of the second phase or duplex grain structures. However, in the XRD patterns as shown in Fig. 5, no peaks of the second phase are observed. When two phase structure occurred, based on the surface tension phenomena, there exists a dihedral angle between the two boundaries that separate the second phase from the first phase, and following the equation listed as:

$$\gamma_{11} = 2\gamma_{12}\cos\frac{\theta}{2} \quad (1)$$

Where, γ_{11} is the surface tension in the first phase boundaries, γ_{12} the surface tension in the two-phase boundary,

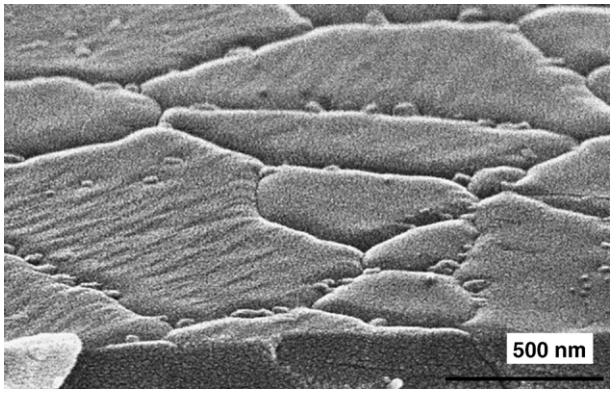

Fig. 4. Surface morphology of the single-cycle furnace annealed $CaCu_3Ti_4O_{12}$ (CCTO) films prepared with 3 coating cycles.

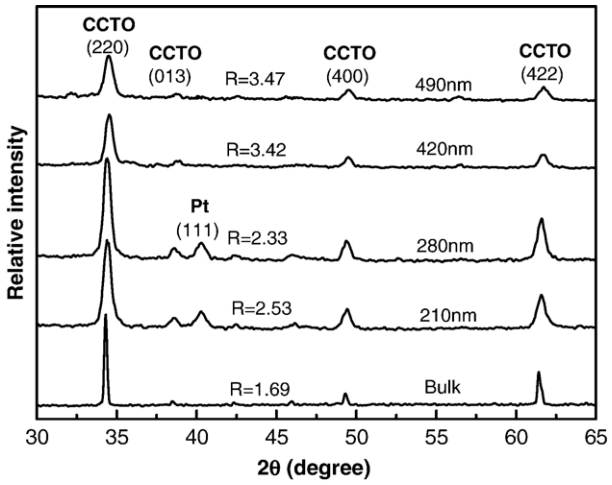

Fig. 5. XRD spectra and peak ratio of Intensity(220)/Intensity(422) (R) of the CCTO thin films with various thicknesses, all the thin films were single-cycle furnace annealed at 800 °C for 30 min. The bulk sample was annealed at 1100 °C for 20 hr in air.

and θ the dihedral angle [11]. With small quantity and large dihedral angle, the second phase tends to form small discrete particles and usually exists in the boundaries of the first phase.

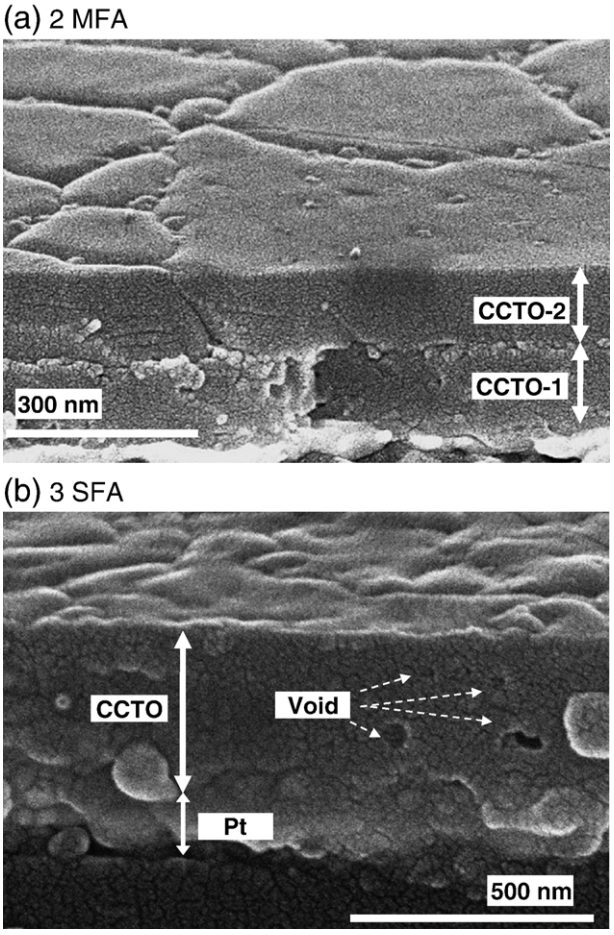

Fig. 6. SEM photographs of the surface and cross-section morphologies of the furnace annealed $CaCu_3Ti_4O_{12}$ (CCTO) thin films prepared with (a) 2 coating cycles and multi-cycle annealing, (b) 3 coating cycles and single-cycle annealing.

The possible second phase grains are also evident in the cross sectional view of CCTO film as seen in Fig. 6, but present in different distribution in samples with SFA and MFA processes. For the sample prepared by SFA process, the second phase distribute randomly in the film surface as shown in Fig. 6(b). However, the second phase grains aggregate at the free surface after each annealing step and form a specific interface between the separated two deposition layers as shown in Fig. 6(a). Fig. 5 shows the X-ray diffraction patterns of the CCTO films by SFA process with different thicknesses on $Pt/Ti/SiO_2/Si$ substrate annealed at 800 °C. No difference is observed for the crystallized CCTO films. For the sample with thinner CCTO films, the Pt (111) peak is appeared in the XRD patterns. The XRD patterns reveal apparent (220), (013), (400), and (422) peaks of CCTO phase, which match the polycrystalline characteristic of the bulk CCTO compounds [12]. According to the XRD pattern of CCTO bulk, the peak ratio $I_{(220)}/I_{(422)}$ is 1.69. However, the $I_{(220)}/I_{(422)}$ ratio for CCTO films are 3.47 (t=490 nm), 3.42 (t=420 nm), 2.33 (t=280 nm), and 2.53 (t=210 nm), which present the characteristic of preferred orientation. The nominal composition of CCTO films is Ca:Cu:Ti:O is 1:3:4:12, but the measured composition is 1:3.75:5.6:21, which indicates the insufficient Ca and excess O constitutions. Though the constitution of the CCTO film deviates from stoichiometry ratio, the phase identification fits the $CaCu_3Ti_4O_{12}$ structure with slightly shifted peaks as shown in Fig. 5. The composition of the second phase is not distinguished from that of the main phase verified by FE-EPMA and TEM-EDX techniques. The TEM image of the sample prepared by SFA process with 3 deposition layers and 280 nm in thickness is shown in Fig. 7. The second phase particles shows growth characteristic as the grains closed to the Pt layer, which implied the heat history will affect the grain sizes of the second phase particles. Some voids are also presented randomly in the TEM observation. A further study on the microstructure, orientation and composition of CCTO film is still under investigation.

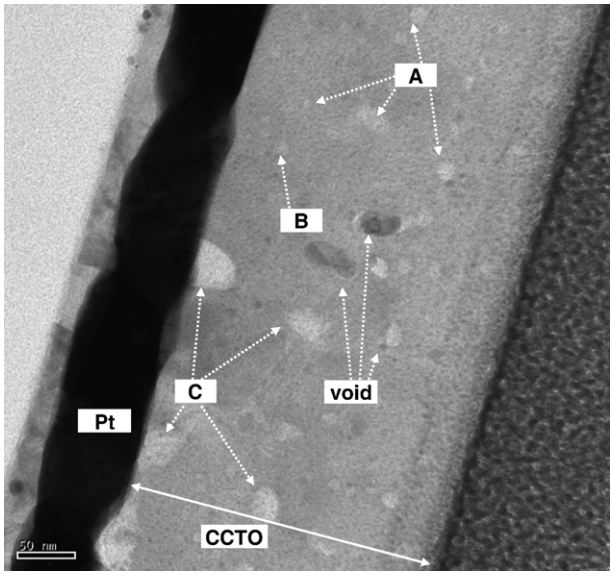

Fig. 7. Cross-sectional TEM of 3MFA-CCTO/Pt, A, B, C are the second-phase grains within the CCTO films.

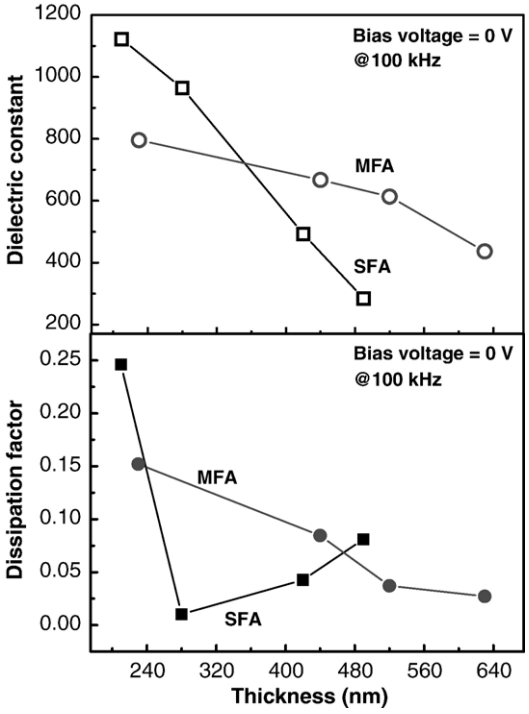

Fig. 8. Dielectric constants and dissipation factor for single-cycle and multi-cycle furnace annealed $CaCu_3Ti_4O_{12}$ (CCTO) films as a function of film thickness.

3.2. Electrical properties

Fig. 8 shows the variation in the dielectric constant and dissipation factor as a function of the film thickness of CCTO films, prepared by single-cycle and multi-cycle furnace annealing, respectively. The dielectric constants of CCTO films prepared by SFA process reveal decreasing trend as the thickness (coating cycle) increases. The film with 210 nm in thickness has a high dielectric constant of near 1120 at 100 kHz, but the film with 490 nm in thickness presents 280 only. The dissipation factor decreases with thickness initially, then increases with thickness when the thickness is above 300 nm. The dielectric constants of the films prepared by MFA-process also exhibit decreasing trend as the thickness increases but with a gentler slope, e.g., 790 at 100 kHz for the 230 nm films, and 430 for the 630 nm films.

The dissipation factor decreases with thickness gradually. The loss of the CCTO films might be caused from voids and/or second phase (interface between the two grains with different grain size). Jiang et al. [8] also estimated that the grain boundary or domain boundary inside the CCTO films play a key role in their dielectric properties. More analyses of the effects of pore diameter, grain size, and film thickness on the dielectric properties are still under investigation.

Moreover, there are two physical structures of the films for these two annealing methods, as shown in Fig. 6. A simplification is to discuss the subject in relation to a system of only two phases. There are CCTO and interlayer within MFA-prepared dielectrics. The case, SFA-prepared dielectrics,

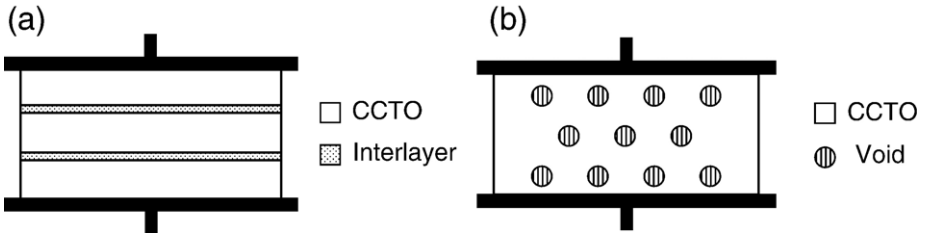

Fig. 9. Possible arrangements of two phases in a mixture with (a) two phases (CCTO and interlayer) in series and are parallel to the specimen electrodes, and (b) random dispersion of void in CCTO matrix.

where phase-1 (CCTO) is continuous and has dispersed in it phase-2 (void) in the form of spheres. The schematics could be shown as Fig. 9(a) and (b). Then, the dielectric constant of the dielectrics could be derived by Mixture Rule as below:

For MFA prepared dielectric:

$$\frac{1}{k} = \frac{v_1}{k_1} + \frac{v_2}{k_2} \tag{2}$$

[13]where k is the dielectric constant of the film, k_1 and k_2 are the dielectric constant of CCTO and interlayer, v_1 and v_2 are the volume fraction of CCTO and interlayer, respectively. As the volume fraction is equal to the relative plate thicknesses, Eq. (2) could be observed:

$$\frac{1}{k} = \frac{x}{k_1} + \frac{(1-x)}{k_2} \tag{3}$$

where x is the ratio of the thickness of CCTO to that of the film.

As shown in Fig. 10(a), this relationship comes very close to linear expression. The dielectric constants of CCTO and interlayer could be derived ($k_{\mathrm{CCTO}} \sim 1910$, $k_{\mathrm{interlayer}} \sim 229$) by linear fitting.

For SFA prepared dielectric:

$$\log k = v_1 \log k_1 + v_2 \log k_2 \tag{4}$$

[14] where k is the dielectric constant of the film, k_1 and k_2 are the dielectric constant of CCTO and void, v_1 and v_2 are the volume fraction of CCTO and void. The volume fraction (v_1) is equal to $(1-x)$ and $k_1 = 1910$, $k_2 = 1$, Eq. (4) could be simplified:

$$\log k = v_1 \log k_1 = (1-x)\log(1910) \tag{5}$$

A pore fraction of dielectric film could be derived as shown in Fig. 10(b). The porosity of the SFA-prepared dielectric increases with the increasing thickness. As the thickness of the film is up to 500 nm, the pore fraction is high as 25% for SFA process.

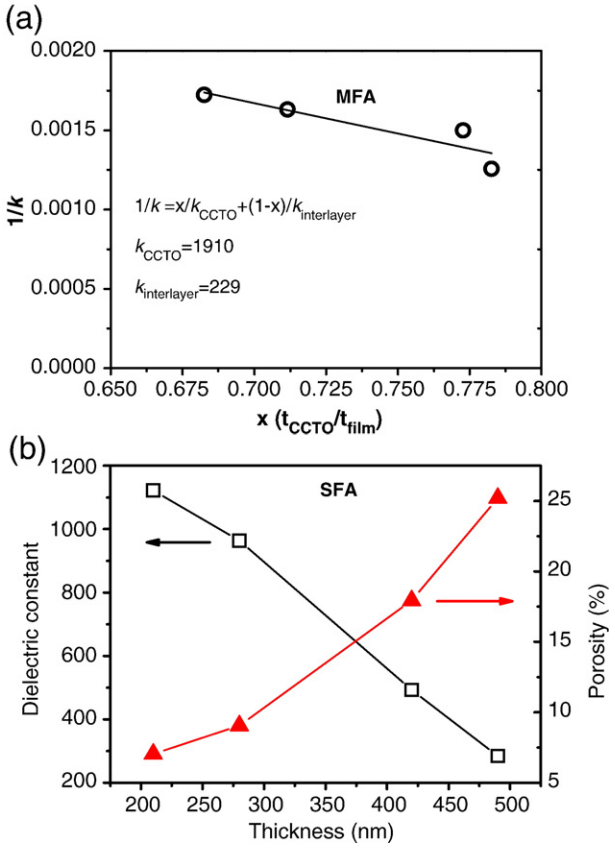

Fig. 10. (a) $1/k$ vs. x (the ratio of the thickness of CCTO to that of the film) plot for multi-cycle furnace annealed $CaCu_3Ti_4O_{12}$ (CCTO) films. (b) Thickness dependent dielectric constant and porosity for single-cycle furnace annealed CCTO films.

4. Conclusions

The dielectric properties of $CaCu_3Ti_4O_{12}$ (CCTO) films prepared by sol–gel process strong depend on the thickness of the films and annealing method. For the sample prepared by single-cycle furnace annealing (SFA) process, the second phase distribute randomly in the dielectric. For the multi-cycle furnace annealing (MFA), the grains of the second phase aggregate at the free surface after each annealing step and form an interface between the successively deposited CCTO layers. The dielectric constants of CCTO and interlayer were derived as ~1910 and ~229, respectively. For SFA process, the porosity of the dielectrics increases with the thickness increasing.

Acknowledgement

This work is sponsored by National Science Council, Taiwan, under the contract number NSC 95-2221-E-009-085.

References

[1] L. Fang, M. Shen, D. Yao, Appl. Phys., A 80 (2005) 1763.
[2] M.A. Subramanian, L. Dong, N. Duan, B.A. Reisner, A.W. Sleight, J. Solid State Chem. 151 (2000) 323.
[3] A.P. Ramirez, M.A. Subramanian, M. Gardel, G. Blumberg, D. Li, T. Vogt, S.M. Shapiro, Solid State Commun. 115 (2000) 217.
[4] A. Koitzsch, G. Blumberg, A. Gozar, B. Dennis, A.P. Ramirez, S. Trebst, S. Wakimoto, Phys. Rev., B 65 (2002) 052406.
[5] L. He, J.B. Neaton, M.H. Cohen, D. Vanderbilt, C.C. Homes, Phys. Rev., B 65 (2002) 214112.
[6] N. Kolev, R.P. Bontchev, A.J. Jacobson, V.N. Popov, V.G. Hadjiev, A.P. Litvinchuk, M.N. Iliev, Phys. Rev., B 66 (2002) 132102.
[7] D.C. Sinclair, T.B. Adams, F.D. Morrison, A.R. West, Appl. Phys. Lett. 80 (2002) 2153.
[8] J.C. Jiang, E.I. Meletis, C.L. Chen, Y. Lin, Z. Zhang, W.K. Chu, Philos. Mag. Lett. 84 (2004) 443.
[9] L. Fang, M. Shen, Thin Solid Films 440 (2003) 60.
[10] L. Fang, M. Shen, J. Appl. Phys. 95 (2004) 6483.
[11] R.E. Reed-Hill, Physical Metallurgy Principles, Second edition, Brooks/Cole Engineering Division, 1973, p. 222.
[12] JCPDS 75-2188.
[13] W.D. Kingery, H.K. Bowen, D.R. Uhlmann, Introduction to Ceramics, Second edition, John Wiley & Sons, 1976, p. 947.
[14] Relva C. Buchanan (Ed.), Ceramic Materials for Electronics: Processing, Properties, and Applications, Marcel Dekker, 1986, p. 85.